Dyes and Pigments 94 (2012) 169–174

Contents lists available at SciVerse ScienceDirect

Dyes and Pigments

journal homepage: www.elsevier.com/locate/dyepig

Synthesis, circular dichroism, and third-order nonlinear optical properties of optically active porphyrin derivatives bearing four chiral citronellal moieties

Jitao Lu [a,b], Lizhen Wu [a], Lu Jing [c], Xiaohong Xu [a], Xiaomei Zhang [a,*]

[a] Department of Chemistry and Chemical Engineering, Shandong University, Jinan 250100, China
[b] Department of Chemistry and Chemical Engineering, Weifang University, Weifang 261061, China
[c] No. 1 Geological and Mineral Exploration Institute of Shandong Province, Jinan 250100, China

ARTICLE INFO

Article history:
Received 28 October 2011
Received in revised form
27 December 2011
Accepted 31 December 2011
Available online 13 January 2012

Keywords:
Porphyrin
Chirality
Chiral information transfer
Third-order nonlinear optical properties
Z-scan
Self-assembly

ABSTRACT

(*R*)-Enantiomer of optically active metal free porphyrin, bearing four chiral citronellal units linked directly onto the meso positions of the porphyrin ring, and its zinc congener, namely (*R*)-*meso*-5,10,15,20-tetra-(2,6-dimethyl-5-heptenyl) porphyrin [(*R*)-$H_2T(C_9H_{17})_4P$ (**1**)] and (*R*)-*meso*-5,10,15,20-tetra-(2,6-dimethyl-5-heptenyl) porphyrinato zinc complex [(*R*)-$ZnT(C_9H_{17})_4P$ (**2**)], have been designed and synthesized. These two compounds were characterized by a wide range of spectroscopic methods. In contrast to the CD silent of a similar compound N,N′,N″-Tris{21H,23H-5-*p*-Aminophenyl-10,15,20-tris-[*p*-(S)-3,7-dimethyloctoxyphenyl]porphyrin}-1,3,5-tricarboxamid, bearing the similar chiral units linked onto the meso positions of the porphyrin ring *via* meso-attached benzene, observation of a positive CD signal in the Soret absorption region of both porphyrin compounds, not only indicate effectively chiral information transfer from the chiral citronellal tails to porphyrin chromophore at the molecular level, but also reveal the effect of substituents position on the asymmetrical perturbation. In addition, both compounds were revealed to show good third-order nonlinear optical properties.

1. Introduction

Chirality is one of the most fascinating and complicated features commonly found in nature [1–5]. Inspired by the elegance of biological supramolecular structures, numerous artificial optically active compounds and their helical supramolecular structures with controlled helicity have been developed depending on various non-covalent interactions [6–16]. Among them, optically active porphyrin derivatives have also attracted increasing attention owing to their wide range of biological relevance and industrial applications in the fields of nonlinear optics and chiral catalysis [17–23]. As a consequence, a number of elaborately designed porphyrin molecules with various chiral substituents such as chiral amino acids and chiral hydrocarbons have been synthesized.

It is worth noting that installing stereocenters onto the periphery of porphyrin molecule just provides a possibility toward fabrication of optically active molecules and helical supramolecular structures. Actually, quite a large number of porphyrin compounds with peripheral substituents containing stereocenters even do not display any CD signal in the whole porphyrin absorption range at the molecular level, due to the weak perturbation from the peripheral substituents with stereocenters to the porphyrin chromophore [24,25]. In a similar manner, many porphyrin derivatives bearing peripheral chiral substituents with stereocenters could only form normal supramolecular structures without exhibiting helicity [26–29]. The delicate interplay of intrinsic intermolecular π–π interaction of porphyrin rings with peripheral chiral substituents was believed to play an important role in increasing the chiral perturbation from the peripheral substituents with stereocenters to the porphyrin chromophore, which in turn will result in the formation of artificial optically active porphyrin derivatives. For example, Shinkai and collaborators prepared a porphyrin derivative carrying four chiral sugar chains [30]. Due to the weak chiral perturbation from sugar chains to the porphyrin chromophore, this compound shows no CD signal in the whole porphyrin absorption range at the molecular level. However, a perfect Cotton effect was observed in the porphyrin Soret band region on aggregate depending on the synergistic interplay of intermolecular π–π interaction between porphyrin rings and hydrogen bonding interaction between sugar chains. Very recently, this group revealed the formation of elemental one-dimensional helices from an optically active porphyrin compound bearing four peripheral chiral binaphthyl moieties, linked at the meso-phenyl substituents through crown ether moieties, depending on the intermolecular

* Corresponding author.
E-mail address: zhangxiaomei@sdu.edu.cn (X. Zhang).

0143-7208/$ – see front matter © 2012 Elsevier Ltd. All rights reserved.
doi:10.1016/j.dyepig.2011.12.015

π–π interaction between porphyrin rings and metal–ligand K–O_{crown} coordination bonds between K^+ and crown units [31]. However, synthesizing optically active porphyrin derivatives and fabricating them into helical supramolecular structures still remains rarely.

In the present paper, we have designed and synthesized a (*R*)-enantiomer of optically active metal free porphyrin, bearing four unsaturated chiral citronellal units linked directly onto the meso positions of the porphyrin ring, and its zinc congener, namely (*R*)-*meso*-5,10,15,20-tetra-(2,6-dimethyl-5-heptenyl) porphyrin [(*R*)-$H_2T(C_9H_{17})_4P$ (**1**)] and (*R*)-*meso*-5,10,15,20-tetra-(2,6-dimethyl-5-heptenyl) porphyrinato zinc complex [(*R*)-$ZnT(C_9H_{17})_4P$ (**2**)], Scheme 1. Their chiral information transfer and expression behavior were comparatively investigated with a similar compound N,N′,N″-Tris{21H,23H-5-*p*-Aminophenyl-10,15,20-tris-[*p*-(S)-3,7-dimethyloctoxyphenyl]porphyrin}-1,3,5-tricarboxamid [32], revealing the effect of substituents position on the asymmetrical perturbation. The present result, representing part of our continuous effort toward designing and preparing chiral porphyrin derivatives, will be helpful on providing new insight into chiral information transfer for synthetic conjugated systems at molecular and also supermolecular level.

2. Experimental

2.1. General information

DMF was freshly distilled just before use. Chloroform was purchased from Tianjin Kermel Co. Column chromatography was carried out on silica gel (Merck, Kieselgel 60, 70–230 mesh) with the indicated eluents.(*R*)-Citronellal (99% ee) was purchased from J&K Chemical Ltd. All the other chemicals were of reagent grade form and used as received without further purification.

2.2. Measurements

^1H NMR spectra were recorded on a Bruker DPX 300 spectrometer (300 MHz) in $CDCl_3$ using the residual solvent resonance of $CHCl_3$ at 7.26 ppm relative to $SiMe_4$ as internal reference. MALDI-TOF mass spectra were detected on a Bruker BIFLEX III ultra-high resolution Fourier transform ion cyclotron resonance (FT-ICR) mass spectrometer with α-cyano-4-hydroxycinnamic acid as matrix. Elemental analyses were performed on an Elementar Vavio El III. Electronic absorption spectra were obtained with a Hitachi U-4100 spectrophotometer. Circular dichroism (CD) measurements were carried out on a JASCO J-810 spectropolarimeter. Fourier transform infrared spectra were recorded in KBr pellets with 2 cm^{-1} resolution using a αALPHA-T spectrometer. Fluorescence spectra were measured on a Multifrequency Phase and Modulation Fluorometer. The fluorescence quantum yields are calculated with their monomers in methanol as standard with the same excitation.

2.3. Materials

2.3.1. Preparation of metal free meso-5,10,15,20-tetra-(2,6-dimethyl-5-heptenyl)porphyrin (*1*)

Pyrrole (0.35 ml, 5.0 mmol) and Citronellal (1.1 ml, 5.0 mmol) were combined in 500 ml of chloroform. After purging the solution for 45 min with N_2, trifluoroacetic acid (0.20 ml) was added. The mixture was stirred under N_2 in the absence of light for 25 h before DDQ (0.86 g, 3.8 mmol) was added. The solution was evaporated under reduced pressure and the residue was chromatographed on

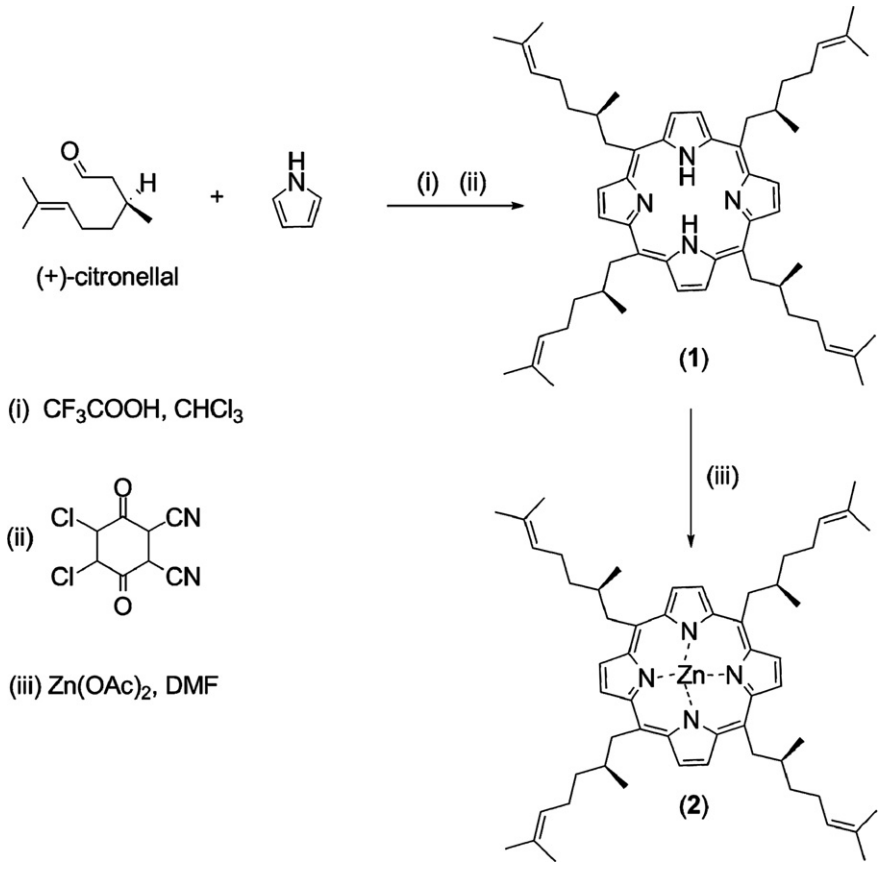

Scheme 1. Synthesis of (*R*)-$H_2T(C_9H_{17})_4P$ (**1**) [(*R*)-$H_2T(C_9H_{17})_4P$ = *meso*-5,10,15,20-tetra-(2,6-dimethyl-5-heptenyl)porphyrin] and its zinc complex (*R*)-$ZnT(C_9H_{17})_4P$ (**2**).

a silica gel column with ethyl acetate/petroleum ether (2:100) as eluent. Repeated chromatography gave pure target compound as a red-brown viscous liquid compound (226 mg, 10%). ^{1}H NMR ($CDCl_3$, 300 MHz): 9.46 (s, 8H, Por-β), 5.02–5.10 (m, 8H, Por-CH_2–), 4.64–4.72 (m, 4H, –CH═), 2.14–2.61 (m, 12H, alkyl), 1.55–1.67 (m, 44H, alkyl), –2.64 (s, 2H, –NH). MS: Calcd. for $C_{56}H_{78}N_4$ 807.2; found *m*/*z* 808.1. Anal. Calcd (%) for $C_{56}H_{78}N_4 \cdot CHCl_3$: C, 73.88; H, 8.59; N, 6.05; found: C, 73.79; H, 8.74; N, 7.24.

2.3.2. Preparation of meso-5,10,15,20-tetra-(2,6-dimethyl-5-heptenyl) porphyrinato zinc complex (**2**)

A mixture of $Zn(OAc)_2 \cdot 2H_2O$ (25 mg, 0.11 mmol) and free meso-5,10,15,20-tetra-(2,6-dimethyl-5-heptenyl)porphyrin (90 mg, 0.11 mmol) in DMF (5 ml) was heated to reflux under nitrogen for ca. 5 h. The solvent was then removed in vacuo and the residue was subjected to chromatography on a silica gel column using 1:100 (v/v) ethyl acetate/petroleum ether (60–90 °C) as eluent. Repeated chromatography gave pure target compound as a dark green compound (82 mg, 85%). ^{1}H NMR (300 MHz): ($CDCl_3$): 9.49 (s, 8H, Por-β), 5.02–5.30 (m, 8H, Por-CH_2–), 4.62–4.70 (m, 4H, –CH═), 2.10–2.66 (m, 12H, alkyl), 1.58–1.68 (m, 44H, alkyl). MS: Calcd. For $C_{56}H_{76}N_4Zn$ 870.6; found *m*/*z* 868.8. Anal. Calcd (%) for $C_{56}H_{76}N_4Zn$: C, 77.25; H, 8.80; N, 6.44; found: C, 77.29; H, 8.61; N, 6.24.

3. Results and discussion

3.1. Molecular design, synthesis, and characterization

As one of the most important typical representative of π-conjugated systems, porphyrin compounds are excellent building blocks to study the chiral information transfer and expression due to their various advantageous, such as the presence of a red-shifted main absorption band (the Soret band at about 418 nm), preventing the overlap with other chromophores absorption below 300 nm, the intense extinction coefficients generally enhancing the sensitivity of CD, facile modification of substituent, and the ease of metal incorporation into the porphyrin ring. Incorporating chiral groups (actually chiral discrimination information) onto the peripheral positions of porphyrin ring therefore provides the possibility to investigate the chiral information transfer and expression from the peripheral chiral units to the central chromophore at molecular level and further the supramolecular level. However, investigation reveals that the peripheral chiral units containing chiral hydrocarbons connected onto the porphyring ring *via* meso-attached benzene usually shows CD inactive in the whole porphyrin absorption range at the molecular level due to the weak asymmetric perturbation [30,32–34]. As a consequence, four (*R*)-citronellal units were incorporated directly onto the meso positions of the porphyrin ligand, Scheme 1, which are expected to enhance the asymmetric perturbation from the peripheral chiral citronellal units to the porphyrin chromophore and result in the formation of optically active porphyrin derivatives.

Metal free porphyrin (*R*)-$H_2T(C_9H_{17})_4P$ (**1**) was synthesized according to published procedure [35]. Its corresponding porphyrinato zinc complex (*R*)-$ZnT(C_9H_{17})_4P$ (**2**) was obtained in good yield from the reaction between (*R*)-$H_2T(C_9H_{17})_4P$ and $Zn(OAc)_2 \cdot 2H_2O$ in refluxing DMF. After repeated column chromatography and recrystallization, satisfactory elemental analysis results were obtained for both newly prepared compounds. These two compounds were also characterized by MALDI-TOF mass spectra and ^{1}H NMR spectroscopy. The MALDI-TOF mass spectra of these two compounds clearly showed intense signals for the protonated molecular ion $[M+H]^+$ for (*R*)-$H_2T(C_9H_{17})_4P$ and $[M-2H]^{2+}$ for (*R*)-$ZnT(C_9H_{17})_4P$, respectively. The isotopic pattern closely resembles the simulated one as exemplified by the spectrum of (*R*)-$H_2T(C_9H_{17})_4P$ given in Figure S1 (Supporting Information). The ^{1}H NMR spectra of compounds (*R*)-$H_2T(C_9H_{17})_4P$ and (*R*)-$ZnT(C_9H_{17})_4P$ have been recorded in $CDCl_3$ at room temperature, Figure S2 (Supporting Information).

3.2. Electronic absorption and circular dichroism (CD) spectroscopy

The electronic absorption spectra and the circular dichroism (CD) of the metal free porphyrin enantiomer **1** and its zinc congener **2** in methanol, are shown in Fig. 1 and the data summarized in Table 1. As expected, both compounds **1** and **2** showed typical features of metal free and porphyrinato metal compounds, respectively, in their electronic absorption spectra, revealing their non-aggregated molecular spectroscopic nature of both compounds in methanol. As can be seen from Fig. 1b, similar to the other metal free porphyrins [36,37], the absorption around 410 nm for the metal free porphyrin enantiomer **1** can be attributed to the porphyrin Soret band, while the four typical weak absorptions at 511, 544, 586, and 640 nm are assigned to Q bands. While complexation with zinc metal ion, the increase in the molecular symmetry from C_{2h} for **1** to D_{2h} for **2** induces change in the electronic absorption spectrum from typical feature for metal free porphyrin to that for typical porphyrinato metal species. As shown in Fig. 1d, the porphyrin Soret and three weak Q bands of complex **2** appeared at 419, 519, 554, and 594 nm, respectively in methanol.

According to the previous research results about the CD spectra of N,N′,N″-Tris{21H,23H-5-*p*-Aminophenyl-10,15,20-tris-[*p*-(S)-3,7-dimethyloctoxyphenyl]porphyrin}-1,3,5-tricarboxamid [32], no CD signal was observed at low concentration (8.3×10^{-6} M), indicating the lack of effective asymmetrical perturbation of the chiral citronellal side chains due to the relatively longer distance between chiral citronellal side chains and porphyrin chloroform. In the present case, when chiral citronellal units were selected to linked directly onto the meso positions of the porphyrin ring instead of *via* meso-attached benzene, the distance between chiral citronellal side chains and porphyrin chromophore are shorten. As a result, as shown in Fig. 1, a positive CD signal in the Soret absorption regions of both porphyrin compounds was appeared (1×10^{-6} M), implying the effective chiral information transfer from the peripheral chiral citronellal side chains to porphyrin chromophore due to the increase of asymmetrical perturbation of the chiral citronellal side chains. According to the chiral exciton theory [38,39], these two compounds are *right*-handed on the basis of the chiral information revealed by the peripheral citronellal units of **1** and **2**.

The electronic absorption and circular dichroism spectra of compounds **1** and **2** in methanol/water [1:1 (v/v)] mixture solvent are also shown in Fig. 1, which are different from the spectra of corresponding compounds in methanol. As shown in Fig. 1b, both the Soret and Q bands of metal free porphyrin **1** in methanol/water [1:1 (v/v)] mixture solvent lose some intensity, with the maximum red-shifting from 410, 511, 544, 586, and 640 nm in methanol to 416, 518, 551, 594, and 650 nm in methanol/water mixture solvent. Similar changes were also observed in the electronic absorption spectrum of zinc porphyrin congener **2**, Fig. 1d. In detail, the Soret band for compound **2** significantly red-shifts from 419 in methanol to 425 nm with the Q bands very slightly red-shifted from 519, 554, and 594 nm in methanol to 520, 556, and 596 nm in methanol/water mixture solvent. On the basis of Kasha's exciton theory [40], red-shifts in the main absorption bands of compounds **1** and **2** upon aggregation indicates the formation of *J*-aggregates depending on the intermolecular π–π interaction between porphyrin molecules, revealing a head-to-tail molecular arrangements in their aggregates. Meantime, in comparison with porphyrin zinc

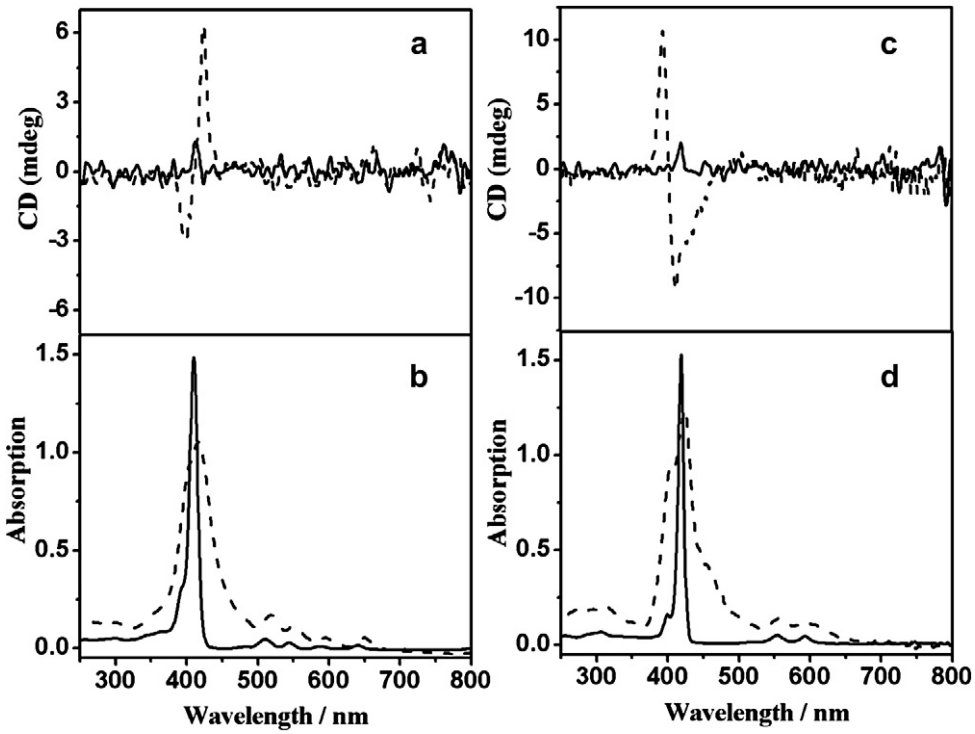

Fig. 1. CD spectra of (*R*)-$H_2T(C_9H_{17})_4P$ (**1**) in dilute methanol solution (solid line) (10^{-6} mol/L) and in the mixture solvent of methanol/water [1:1 (v/v), dashed line] (a); electronic absorption spectrum of (*R*)-$H_2T(C_9H_{17})_4P$ (**1**) and in dilute methanol solution (solid line) and in the mixture solvent of methanol/water [1:1 (v/v), dashed line] (b); CD spectra of (*R*)-$ZnT(C_9H_{17})_4P$ (**2**) in dilute methanol solution (solid line) (10^{-6} mol/L) and in the mixture solvent of methanol/water [1:1 (v/v), dashed line] (c); electronic absorption spectrum of (*R*)-$ZnT(C_9H_{17})_4P$ (**2**) and in dilute methanol solution (solid line) and in the mixture solvent of methanol/water [1:1 (v/v), dashed line] (d).

congener **2**, observation of larger degree red-shift in the Q bands of **1** upon aggregation indicates stronger intermolecular interaction in the direction perpendicularly to the porphyrin rings.

In the CD spectra of compound **1** as well as **2** in methanol/water mixture solvent, Fig. 1a and c, one remarkable bisignate Cotton effect was observed in the porphyrin Soret band region. According to the semiempirical method developed by Nakanishi and co-workers [41–44], the given sign of coupling and the direction of dipole moments can be used to determine the chirality of stacked porphyrin molecules in aggregates. In general, the CD spectrum featuring a bisignate Cotton effect showing positive feature at longer wavelength and negative one at shorter wavelength indicates the right-handed chirality of the dipole moments (positive chirality), while conversely left-handed chirality (negative chirality). In the present case, compounds **1** and **2** display a positive and negative bisignated Cotton effect, {[399(−)/424(+)] for **1** and [411(−)/393(+)] for **2**}, respectively, with the crossover at 420 and 407 nm, corresponding to the Soret band of **1** and **2** aggregates. As a consequence, the positive chirality of aggregates fabricated from **1** in methanol/water mixture solvent corresponds to a *right*-handed helical arrangement and the negative chirality of aggregates fabricated from **2** in methanol/water mixture solvent indicates a *left*-handed helical arrangement of corresponding molecules in a stack of porphyrin chromophores in aggregates. These results confirm chiral information was further amplified and in turn successfully expressed on the porphyrin chromophore at the supramolecular level.

Table 1
Electronic absorption spectral data of complexes **1**–**2** in methanol and corresponding aggregations in methanol/water mixture solvent.

Compound	Methanol	Mathanol/water
1	410, 511, 544, 586, 640	416, 518, 551, 594, 650
2	419, 519, 554, 594	425, 520, 556, 596

3.3. Fluorescence spectra

The fluorescence spectra of porphyrin derivatives are also sensitive to the aggregation. Therefore, the fluorescence spectra measurement is another powerful tool for the investigation of porphyrin derivatives self-aggregation as well as the electronic absorption spectra. The fluorescence spectra of compounds **1** and **2**, measured in methanol and methanol/water mixture solvents are shown in Fig. 2. The fluorescence quantum yields were calculated by using tetraphenylporphyrin in benzene as standard [45]. Fluorescence quantum yields for compounds **1** and **2** in methanol/water mixture solvents are calculated as 42% and 35%, respectively. This relatively strong fluorescence quenching for these two porphyrin compounds in methanol/water mixture solvents compared with that in methanol might be ascribed to the formation of *J*-aggregates, indicating the formation of aggregates with intensified intermolecular π–π interactions between porphyrin rings of the molecules for these two compounds. In addition, compared with the fluorescence spectra of compound **2**, observation of larger degree fluorescence quenching for **1** in methanol/water mixture solvents obviously suggests the formation of aggregates with enhanced π–π interaction between porphyrin **1** rings. This result is in line with the electronic absorption spectra result as detailed above, Fig. 1.

3.4. Nonlinear optical properties

In order to explore the applications for optical limiting, the third-order nonlinear absorption and refraction of compounds **1**

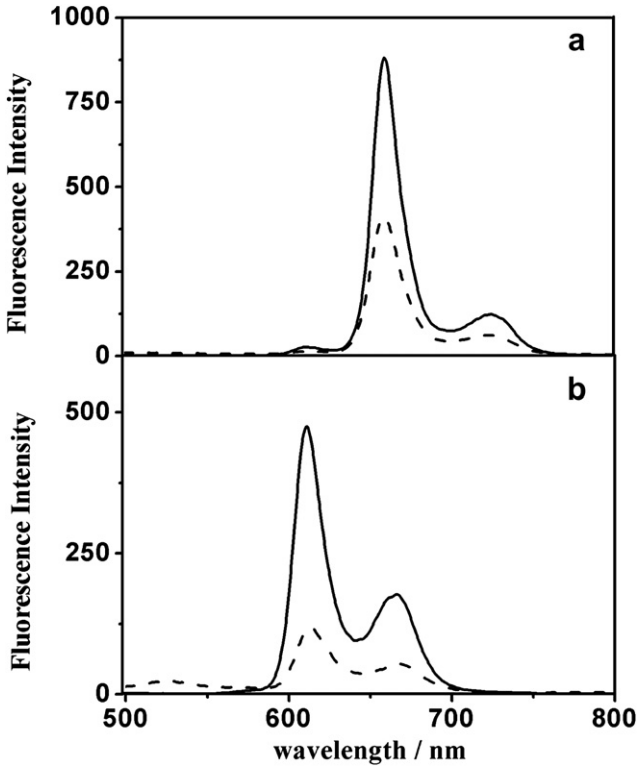

Fig. 2. Fluorescence spectra of (*R*)-$H_2T(C_9H_{17})_4P$ (**1**) in dilute methanol solution (solid line) and in the mixture solvent of methanol/water [1:1 (v/v), dashed line] (λ_{ex} = 421 nm, the absorption at the excitation wavelength was normalized) (a); Fluorescence spectra of (*R*)-$ZnT(C_9H_{17})_4P$ (**2**) in dilute methanol solution (solid line) and in the mixture solvent of methanol/water [1:1 (v/v), dashed line] (λ_{ex} = 429 nm, the absorption at the excitation wavelength was normalized) (b).

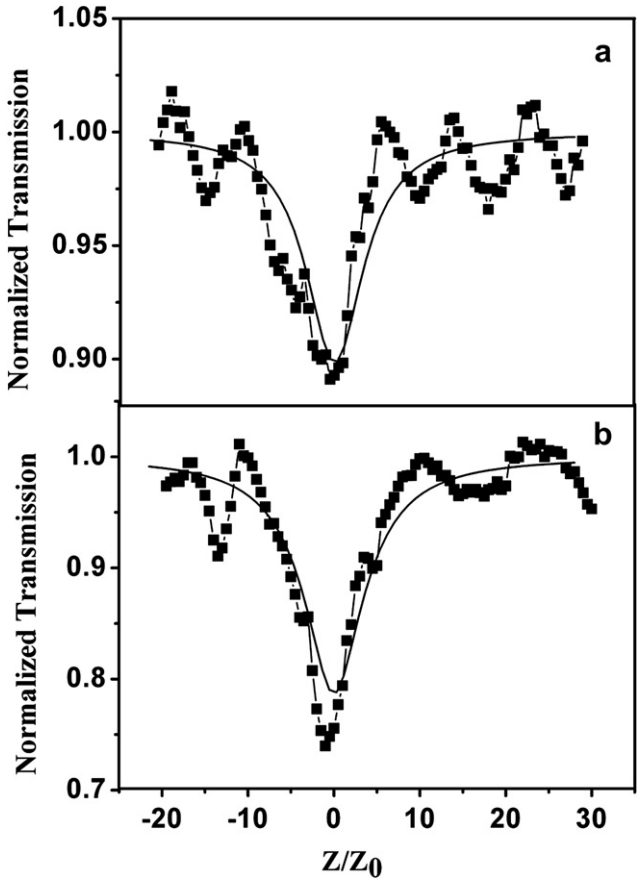

Fig. 3. Z-scan data for (*R*)-$H_2T(C_9H_{17})_4P$ (**1**) and (*R*)-$ZnT(C_9H_{17})_4P$ (**2**) in 10^{-4} mol L^{-1} methanol solution obtained under an open aperture configuration. The black dots are the experimental data and the solid curves are the theoretical fit.

and **2** were measured using the Z-scan technique. Before the measurement, the system was calibrated using CS_2 in a quartz cell as reference. In the measurements, a mode-locked Nd:YAG laser system (PY61C-10, Continuum) was used at the wavelength of 1064 nm with the pulse width of 20 ps and the repetition rate of 10 Hz. The laser beam was focused with an $f = 15$ cm lens and the beam waist radius (w_0) was measured to be 40.0 μm and the corresponding Rayleigh length is 3.9 mm. The thickness of a quartz cell containing the sample is 1 mm which is less than the Rayleigh length of the laser beam. It is noteworthy that the measurements on the pure methanol solvent in the cell were also performed under the same measurement conditions to verify that the valleys and the peaks in the Z-scan curves originated from the material instead from the solvent or the quartz cell.

The NLO absorption components of the metal free porphyrin **1** and its zinc porphyrinato **2** were obtained by a Z-scan experiment under an open aperture configuration and the concentrations of the samples were 1×10^{-4} mol/L. The NLO absorption data can be well represented by equations which describe a third-order NLO absorption process [46]. The NLO absorptive properties of the metal free porphyrin **1** and its zinc congener **2** are shown in Fig. 3. As can be seen two positive nonlinear absorption spectra were observed, which is regarded as two photon absorption (TPA) in the compounds **1** and **2** [47]. The two photon absorption coefficients β of the metal free porphyrin **1** and its zinc congener **2** were calculated to be 8.8×10^{-12} and 2.4×10^{-11} m/W, respectively, which are not weaker than that of other porphyrin derivatives [48–50], indicating the potential application of the two compounds as optical limiting materials.

4. Conclusion

In summary, we have designed and synthesized a (*R*)-enantiomer of optically active metal free porphyrin, bearing four chiral citronellal units linked directly onto the meso positions of the porphyrin ring, and its zinc congener. Compared with the CD silent of N,N′,N″-Tris{21H,23H-5-*p*-Aminophenyl-10,15,20-tris-[*p*-(S)-3,7-dimethyloctoxyphenyl]porphyrin}-1,3,5-tricarboxamid, bearing similar chiral units linked onto the meso positions of the porphyrin ring *via* meso-attached benzene, both compounds show a positive CD signal in the Soret absorption region of both porphyrin compounds, indicating effective chiral information transfer from the chiral citronellal tails to porphyrin chromophore at the molecular level. The present result not only reveals the effect of substituents position on the asymmetrical perturbation but also is helpful on providing new insight into chiral information transfer and expression for synthetic conjugated systems at molecular and supramolecular level.

Acknowledgments

Financial support from the Natural Science Foundation of China (Grant No. 21171106 and 21176144) and Independent Innovation Foundation of SDU.

Appendix. Supplementary material

Supplementary material associated with this article can be found free of charge *via* internet at http://www.elsevier.com/locate/dyepig or from the authors, and at doi:10.1016/j.dyepig.2011.12.015.

References

[1] Garoff RA, Litzinger EA, Connor RE, Fishman I, Armitage BA. Helical aggregation of cyanine dyes on DNA templates: effect of dye structure on formation of homo- and heteroaggregates. Langmuir 2002;18:6330–7.

[2] Wang M, Silva GL, Armitage BA. DNA-templated formation of a helical cyanine dye J-aggregate. J Am Chem Soc 2000;122:9977–86.

[3] Pasternack RF, Giannetto A, Pagano P, Gibbs EJ. Self-assembly of porphyrins on nucleic acids and polypeptides. J Am Chem Soc 1991;113:7799–800.

[4] Hannah KC, Armitage BA. DNA-templated assembly of helical cyanine dye aggregates: a supramolecular chain polymerization. Acc Chem Res 2004;37:845–53.

[5] Chen X, Liu MJ. Induced chirality of binary aggregates of oppositely charged water-soluble porphyrins on DNA matrix. Inorg Biochem 2003;94:106–13.

[6] Schmuck C. Molecules with helical structures: how to build a molecular spiral staircase? Angew Chem Int Ed 2003;42:2448–52.

[7] Nelson JC, Saven JG, Moore JS, Wolynes PG. Solvophobically driven folding of nonbiological oligomers. Science 1997;277:1793–6.

[8] Cornelissen JJLM, Fisher M, Sommerdijk NAJM, Nolte RJM. Helical superstructures from charged poly(styrene)-poly(isocyanodipeptide) block-copolymers. Science 1998;280:1427–30.

[9] Oda R, Schmutz M, Candau SJ, MacKintosh FC. Tuning bilayer twist using chiral counterions. Nature 1999;399:566–9.

[10] Hirschberg JHKK, Brunsveld L, Ramzi A, Vekemans JAJM, Sijbesma RP, Meijer EW. Helical self-assembled polymers via cooperative stacking of hydrogen-bonded pairs. Nature 2000;407:167–70.

[11] Berl V, Huc I, Khoury RG, Krische MJ, Lehn J-M. Interconversion of single and double helices formed from synthetic molecular strands. Nature 2000;407:720–3.

[12] Zubarev ER, Pralle MU, Sone ED, Stupp SI. Self-assembly of dendron rodcoil molecules into nanoribbons. J Am Chem Soc 2001;123:4105–6.

[13] Sone ED, Zubarev ER, Stupp SI. Semiconductor nanohelices templated by supramolecular ribbons. Angew Chem Int Ed 2002;41:1705–9.

[14] Fenniri H, Deng B-L, Ribbe AE. Helical rosette nanotubes with tunable chiroptical properties. J Am Chem Soc 2002;124:11064–72.

[15] Giorgi T, Lena S, Mariani P, Cremonini MA, Masiero S, Pieraccini S, et al. Supramolecular helices via self-assembly of 8-oxoguanosines. J Am Chem Soc 2003;125:14741–9.

[16] Xiao J, Xu J, Cui S, Liu H, Wang S, Li Y. Supramolecular helix of an amphiphilic pyrene derivative induced by chiral tryptophan through electrostatic interactions. Org Lett 2008;10:645–8.

[17] Ogoshi H, Mizutani T. Multifunctional and chiral porphyrins: model receptors for chiral recognition. Acc Chem Res 1998;31:81–9.

[18] Huang X, Nakanishi K, Berova N. Porphyrins and metalloporphyrins:versatile circular dichroic reporter groups for structural studies. Chirality 2000;12:237–55.

[19] Huang X, Richman BH, Borhan B, Berova N, Nakanishi K. Zinc porphyrin tweezer in host–guest complexation: determination of Absolute configurations of diamines, amino acids, and amino alcohols by circular dichroism. J Am Chem Soc 1998;120:6185–6.

[20] Proni G, Pescitelli G, Huang X, Nakanishi K, Berova N. Magnesium tetraarylporphyrin tweezer: a CD-sensitive host for absolute configurational assignments of α-chiral carboxylic acids. J Am Chem Soc 2003;125:12914–27.

[21] Kurtán T, Nesnas N, Li Y, Huang X, Nakanishi K, Berova N. Chiral recognition by CD-sensitive dimeric zinc porphyrin host. 1. Chiroptical protocol for absolute configurational assignments of monoalcohols and primary monoamines. J Am Chem Soc 2001;123:5962–73.

[22] Kurtán T, Nesnas N, Koehn FE, Li Y, Nakanishi K, Berova N. Chiral recognition by CD-sensitive dimeric zinc porphyrin host. 2. Structural studies of host–-guest complexes with chiral alcohol and monoamine conjugates. J Am Chem Soc 2001;123:5974–82.

[23] Borovkov VV, Lintuluoto JM, Sugiura M, Inoue Y, Kuroda R. remarkable stability and enhanced optical activity of a chiral supramolecular bisporphyrin tweezer in both solution and solid state. J Am Chem Soc 2002;124:11282–3.

[24] Tamaru S, Takeuchi M, Sano M, Shinkai S. Sol–gel transcription of sugar-appended porphyrin assemblies into fibrous silica: unimolecular stacks versus helical bundles as templates. Angew Chem Int Ed 2002;41:853–6.

[25] Tamaru S-I, Nakamura M, Takeuchi M, Shinkai S. Rational design of a sugar-appended porphyrin gelator that is forced to assemble into a one-dimensional aggregate. Org Lett 2001;3:3631–4.

[26] Guo XM, Jiang C, Shi TS. Prepared chiral nanorods of a cobalt(II) porphyrin dimer and studied changes of UV–Vis and CD spectra with aggregate morphologies under different temperatures. Inorg Chem 2007;46:4766–8.

[27] Fuhrhop J-H, Demoulin C, Boettcher C, Köning J, Siggels U. Chiral micellar porphyrin fibers with 2-aminoglycosamide head groups. J Am Chem Soc 1992;114:4159–69.

[28] Arimori S, Takeuchi M, Shinkai S. Sugar-controlled aggregate formation in boronic acid-appended porphyrin amphiphiles. J Am Chem Soc 1996;118:245–6.

[29] Ishi-I T, Jung JH, Shinkai S. Intermolecular porphyrin–fullerene interactioncan reinforce the organogel structure of a porphyrin-appended cholesterolderivative. J Mater Chem 2000;10:2238–40.

[30] Tamaru S, Uchino S, Takeuchi M, Ikeda M, Hatano T, Shinkai S. A porphyrin-based gelator assembly which is reinforced by peripheral urea groups and chirally twisted by chiral urea additives. Tetrahedron Lett 2002;43:3751–5.

[31] Lu J, Wu L, Jiang J, Zhang X. Helical nanostructures of an optically active metal-free porphyrin with four optically active binaphthyl moieties: effect of metal–ligand coordination on the morphology. Eur J Inorg Chem; 2010:4000–8.

[32] Hameren R, van Buul AM, Castriciano MA, Villari V, Micali N, Schön P, et al. Supramolecular porphyrin polymers in solution and at the solid–liquid interface. Nano Lett 2008;8:253–9.

[33] Monti D, Venanzi M, Stefanelli M, Sorrenti A, Mancini G, Natale C, et al. Chiral amplification of chiral porphyrin derivatives by templated heteroaggregation. J Am Chem Soc 2007;129:6688–9.

[34] Hoeben F, Wolffs M, Zhang J, Feyter S, Leclère P, Schenning A, et al. Influence of supramolecular organization on energy transfer properties in chiral oligo(p-phenylene vinylene) porphyrin assemblies. J Am Chem Soc 2007;129:9819–28.

[35] Fox MA, Grant JV, Melamed D, Torimoto T, Liu C, Bard AJ. Effect of structural variation on photocurrent efficiency in alkyl-substituted porphyrin solid-state thin layer photocells. Chem Mater 1998;10:1771–6.

[36] Ulman A, Manassen J. Synthesis of new tetraphenylporphyrin molecules containing heteroatoms other than nitrogen. I. Tetraphenyl-21,23-dithiaporphyrin. J Am Chem Soc 1975;97:6540–4.

[37] Lu G, Zhang X, Cai X, Jiang J. Tuning the morphology of self-assembled nanostructures of amphiphilic tetra(p-hydroxyphenyl)porphyrins with hydrogen bonding and metal–ligand coordination bonding. J Mater Chem 2009;19:2417–24.

[38] Harada H, Nakanishi K. Circular dichroic spectroscopy, exciton coupling in organic stereochemistry. New York: University Science Books; 1983.

[39] Kobayashi N. Optically active 'adjacent' type non-centrosymmetrically substituted phthalocyanines. Chem Commun; 1998:487–8.

[40] Kasha M, Rawls HR, El-Bayoumi MA. The exciton model in molecular spectroscopy. Pure Appl Chem 1965;11:371–92.

[41] Berova N, Nakanishi K, Woody R. Circular dichroism: princples and applications. 2nd ed. New York: Wiley-VCH; 2000. pp. 337–82.

[42] Hofacker AL, Parquette JR. Dendrimer folding in aqueous media: an example of solvent-mediated chirality switching. Angew Chem Int Ed 2005;44:1053–7.

[43] Balaz M, Holmes AE, Benedetti M, Rodriguez PC, Berova N, Nakanishi K, et al. Synthesis and circular dichroism of tetraarylporphyrin–oligonucleotide conjugates. J Am Chem Soc 2005;127:4172–3.

[44] Borovkov VV, Lintuluoto JM, Fujiki M, Inoue Y. Temperature effect on supramolecular chirality induction in bis(zinc porphyrin). J Am Chem Soc 2000;122:4403–7.

[45] Feng J, Liang B, Wang D, Wu H, Xue L, Li X. Synthesis and aggregation behavior of perylenetetracarboxylic diimide trimers with different substituents at bay positions. Langmuir 2008;24:11209–15.

[46] Sheik-Bahae M, Said AA, Wei TH, Hagan DJ, Van Stryland EW. Sensitive measurement of optical nonlinearities using a single beam. IEEE J Quantum Electron 1990;26:760–9.

[47] Terazima M, Shimizu H, Osuka A. The third order nonlinear optical properties of porphyrin oligomers. J Appl Phys 1997;81:2946–51.

[48] Senge MO, Fazekas M, Notaras EGA, Blau WJ, Zawadzka M, Locos OB, et al. Nonlinear optical properties of porphyrins. Adv Mater 2007;19:2737–47.

[49] Kandasamy K, Shetty SJ, Puntambekar PN, Srivastava TS, Kundu T, Singh BP. Effects of metal substitution on third-order optical non-linearity of porphyrin macrocycle. J Porphyrins Phthalocyanines 1999;3:81–6.

[50] de la Torre G, Vzquez P, Agull-Lpez F, Torres T. Role of structural factors in the nonlinear optical properties of phthalocyanines and related compounds. Chem Rev 2004;104:3723–50.